Protonation Energies of 1–5-Ring Polycyclic Aromatic Nitrogen Heterocyclics: Comparing Experiment and Theory

ARTICLE *in* THE JOURNAL OF PHYSICAL CHEMISTRY A · DECEMBER 2014

Impact Factor: 2.69 · DOI: 10.1021/jp506913r · Source: PubMed

6 AUTHORS, INCLUDING:

Michael Noah Mautner
Virginia Commonwealth University
202 PUBLICATIONS **5,307** CITATIONS

THE JOURNAL OF PHYSICAL CHEMISTRY A

Article

pubs.acs.org/JPCA

Protonation Energies of 1−5-Ring Polycyclic Aromatic Nitrogen Heterocyclics: Comparing Experiment and Theory

Alexander Wiseman,[†] Lacey A. Sims,[†] Russell Snead,[†] Scott Gronert,*[,†] Robert G. A. R. Maclagan,[‡] and Michael Meot-Ner (Mautner)*[,†,‡]

[†]Department of Chemistry, Virginia Commonwealth University, Richmond, Virginia 23284-2006, United States

[‡]Department of Chemistry, University of Canterbury, Private Bag 4800, Christchurch 8140, New Zealand

ABSTRACT: Polycyclic nitrogen heterocyclic compounds (PANHs) can be protonated in the gas phase in mass spectrometry, in solution in acidic and biological environments, and if present, in interstellar clouds. Intrinsic molecular effects on PANH basicities can be observed by their gas phase protonation thermochemistry. We determined the gas phase basicities/proton affinities (GBs/PAs) of prototype one-nitrogen, 3−5-ring PANH compounds of increasing sizes and polarizabilities by kinetic bracketing, using proton transfer reactions to reference bases. The experimental proton affinities increase from 1-ring (pyridine, 222.2); to 2-ring (quinoline, 227.8); to 3−5-ring compounds, 227−234 kcal mol^{-1}. We also calculated the GB/PA values at the M06-2X/6-311+G**//B3LYP/6-31g* level. The computed PAs agree, within the experimental uncertainty, with the experimental values anchored to the upper range of the NIST GB/PA database. Specifically, the computed PAs are smaller than the experimental values by 1.4 ± 0.9 kcal/mol for nonaromatic nitrogen reference bases and for 1−5-ring PANHs, independently of the number of rings, aromaticity, and molecular size. Therefore, a useful method to calculate proton affinities of PANH compounds can use M06-2X/6-311+G**//B3LYP/6-31g* computational PAs + 1.4 ± 0.9 kcal mol^{-1}. The agreement with experiment supports the NIST database within this accuracy, in the upper range up to 235 kcal mol^{-1}, even though there are no direct absolute experimental anchor points in this range. For astrochemical applications, the measured PAs allow calculating the energies of the $(PANH)^{+\bullet} + H_2 \rightarrow (PANH)H^+ + H^\bullet$ reactions that may convert the radical ions to less reactive 11-electron ions. The reactions are endothermic or nearly thermoneutral for the 3−5-ring ions and would be very slow at low temperatures, allowing reactive $(PANH)^{+\bullet}$ radical ions to persist in interstellar clouds.

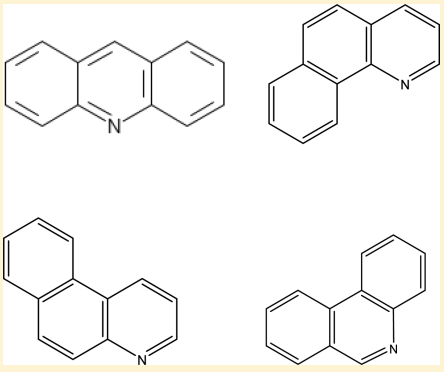

INTRODUCTION

Polycyclic aromatic nitrogen heterocyclic (PANH) compounds participate in a wide range of phenomena in biological, environmental, industrial, and possibly interstellar chemistry. PANHs are strong bases in the gas phase where they can be protonated in mass spectrometry and in space and can be protonated also in the condensed phase in low pH solutions. Gas-phase basicities (GB) and proton affinities (PA) can reveal the molecular factors in protonation thermochemistry, and comparison with solution can quantify solvation effects.[1−3]

The protonation thermochemistry of aromatic nitrogen heterocyclics have been measured for compounds with various substituents, such as pyridine derivatives,[4,5] proton sponges,[6] and nucleic bases.[7] Unsubstituted PANHs can also occur in nature. They have been suggested in interstellar clouds[8−11] and serve as ligands in supramolecular complexes.[12] Also, PANH properties may be extrapolated to nitrogen-doped graphene, where nitrogen atoms in graphene sheets create pyridine-like positions at sheet edges.[12]

Despite these interests, the gas-phase protonation thermochemistry of unsubstituted PANHs has been measured only for the smallest compounds pyridine, quinoline, isoquinoline, and acridine,[1−3,7,13,14] in part because the low volatility of larger compounds prevents proton transfer equilibrium studies. However, the protonated ions can be now produced by electrospray ionization mass spectrometry, and the proton affinities can be obtained then by bracketing methods.

The protonation thermochemistry can also be calculated theoretically. We shall compare the calculated GB/PA results with experiment for a set of PANH's to evaluate the computations, which can be then extended to further PANH compounds that are hard to obtain or produce. This paper compares experiment with theory for several 2−5-ring PANHs, and a larger set of compounds was also computed.[15]

EXPERIMENTAL METHODS

A Bruker Esquire quadrupole ion trap mass spectrometer was used to obtain the proton affinities of the PANHs shown in Figure 1.

The method consists of measuring the second-order proton transfer rate coefficients k_{PT} and reaction efficiencies $r_1 = k_{PT}/k_{collision}$ of proton transfer reactions from the protonated

Received: July 11, 2014
Revised: October 14, 2014
Published: December 5, 2014

DOI: 10.1021/jp506913r
J. Phys. Chem. A 2015, 119, 118−126

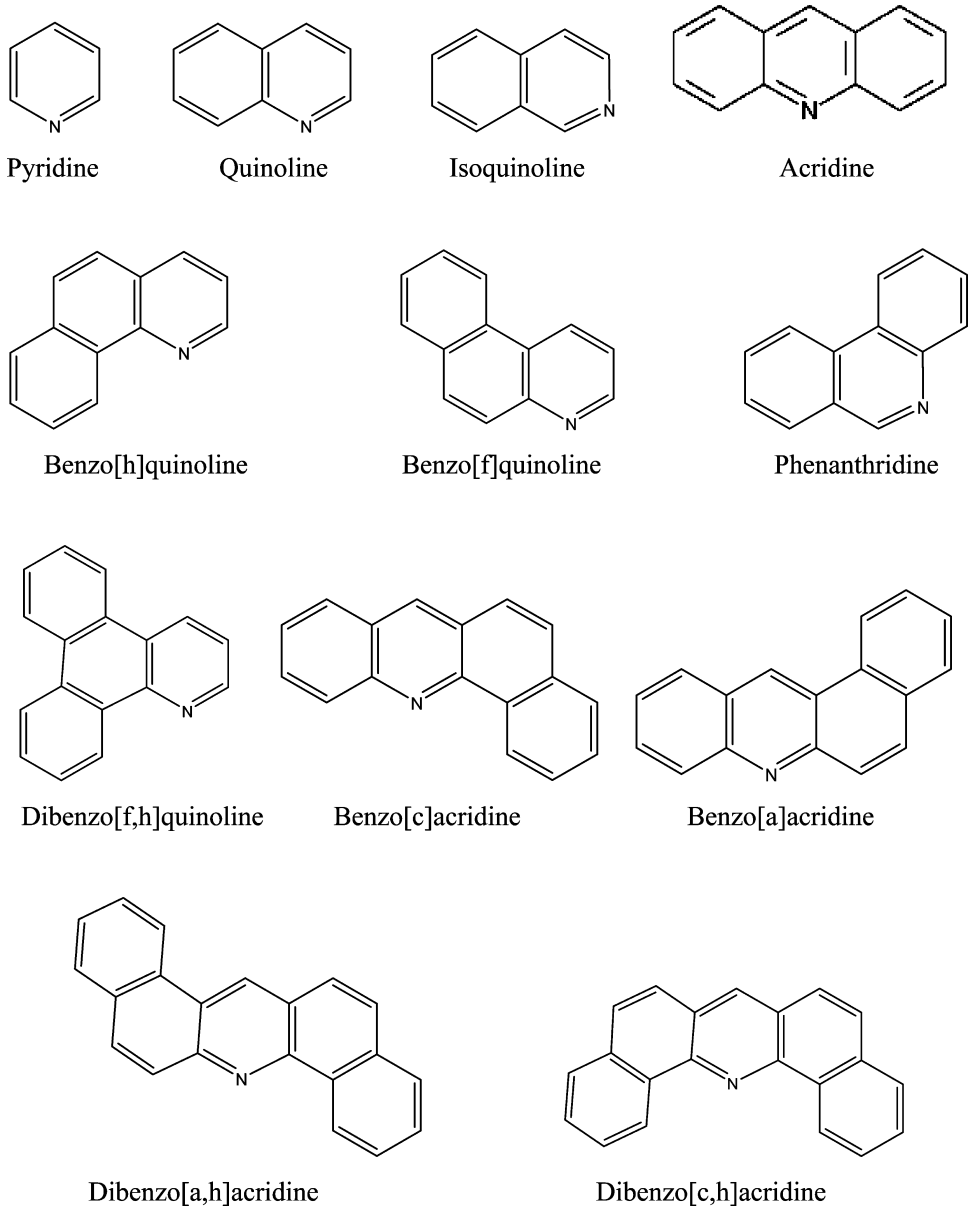

Figure 1. Structures of the compounds in this work.

compounds MH^+ of interest to a series of reference compounds B that have known gas-phase basicities (GB) (reaction 1).

$$MH^+ + B \rightarrow BH^+ + M \quad (1)$$

The experimental methods are analogous to those used in several studies with ThermoFinnigan ion traps in our laboratories.[16−18] Ions were generated by electrospray ionization of ∼10^{-5} M solutions of appropriate precursors in methanol (flow rates ranging from 2.67−2.83 μL/min or 160−170 μL/h). Typical ESI conditions involved needle potentials from 3.5 to 3.9 kV and heated capillary temperatures from 125 to 200 °C. After a short time delay in which ions were collected, a notched waveform was applied to isolate the ion of interest in the ion trap. Once a steady signal was achieved, the neutral reagent reference base B was introduced into the helium buffer gas via a custom gas-handling system. This was done by injecting a constant flow of reagent B (50−200 μL/h) by a syringe pump with the syringe's needle being directed into a measured flow of helium (1000 mL/min). This process allows for rapid vaporization at the needle yielding mixing ratios of 10^3−10^5 (He/B). In some cases, B was diluted in toluene to allow for higher He/B ratios with reasonable reagent flow rates. Most of the gas is then discarded through a flowmeter, whereas a small amount (∼0.1 mL/min) is transferred into the trap. To control the helium pressure, a constriction capillary was used to control the flow and maintain a pressure (He + B) of about 0.01 mTorr in the trap. When combined with the mixing ratio, the ion trap pressure can be used to calculate the reagent's partial pressure (a differential effusion correction is needed). The ion trap pressure was routinely calibrated by collecting data for reactions with established rate constants. Once an appropriate flow of the neutral reagent was established, the system was given several minutes for the reagent pressure to equilibrate to a steady state. To analyze the reactions, the ion traps were set to do a tandem mass spectrometry (MS/MS) scan with no excitation energy and a varying excitation time. Reactions were monitored as a function of time at various flow rates (pressures) of the reagent B. Kinetic measurements were

DOI: 10.1021/jp506913r
J. Phys. Chem. A 2015, 119, 118−126

Table 1. Experimental Rate Coefficients for $MH^+ + B \rightarrow BH^+ + M$ and Proton Affinities (PA) of B and M[a,b]

		sample compound (M)							
reference base (B)	PA(B) (NIST)	benzo[*h*] quinoline (228.0)	benzo[*f*] quinoline (228.6)	dibenzo[*f*,*h*]quinoline (228.9)	phenanthridine (228.5)	acridine (232.4)	benzo[*c*] acridine (232.5)	dibenzo[*c*,*h*]acridine (233.0)	benzo[*a*] acridine (234.2)
4-methylpyridine (4-p)	226.4	0.07							
2-methylpyridine (2-p)	226.8			0.01					
2-ethylpyridine (2-ep)	227.6	0.25			0.05				
quinoline (quin)	227.8	**0.06**							
piperidine (pip)	228.0	0.29		**0.06**	0.06				
3,5-lutidine (3,5-L)	228.3		**0.18**						
2,5-lutidine (2,5-L)	229.2	**1.09**	**0.44**		**0.21**				
N,*N*-dimethylethylamine (n,n-de)	229.5	0.63		**0.39**	0.20				
2,4-lutidine (2,4-L)	230.1	1.17	0.86	0.64	**0.86**	0.02			
1-methylpyrrolidine (1-my)	230.8			0.75	0.74	0.04			
dibutylamine (dib)	231.5			1.04	1.19				
N,*N*-dimethylbutylamine (n,n-db)	231.6			0.93		0.08	0.07		
N,*N*-dimethyl isopropylamine (n,n-di)	232.0			0.95		**0.16**	**0.13**		**0.02**
1-methylpiperidine (1-mp)	232.1			0.84		0.15	0.13	**0.07**	0.02
triethylamine (te)	234.7			0.93	1.09	**0.80**	**0.73**	0.40	0.37
N,*N*-dimethylcyclohexylamine (n,n-dc)	235.1			1.08		0.89	0.76	**0.69**	**0.35**
tripropylamine (tp)	236.9			1.20		1.11			1.7

[a]PAs in kcal mol^{-1}. The proton affinities of the reference compounds, PA(B), are from the NIST Webbook databases (refs 13 and 14). The assigned experimental PAs under compound name in the top row are from the present work. [b]Rate coefficients in 10^{-9} cm^3 $molecule^{-1}$ s^{-1}. The rate coefficients in bold were interpolated to 0.25 cm^3 $molecule^{-1}$ s^{-1} where proton transfer is considered ergoneutral or thermoneutral, and the corresponding value on the abscissa is considered as PA(B). Standard deviations in replicate rate coefficient measurements were typically less than ±5%, but absolute uncertainties are estimated as the usual ±30% for ion−molecule rate coefficient measurements.

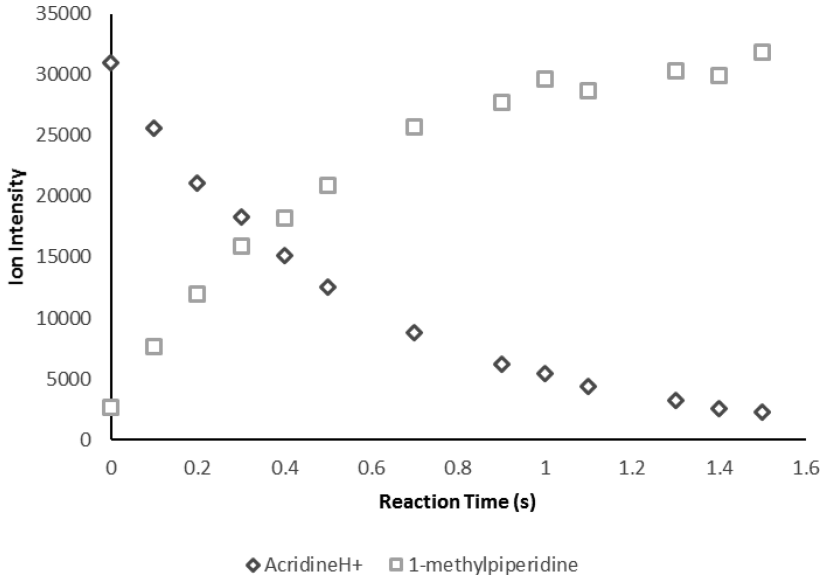

Figure 2. Ion signal intensities as a function of reaction time in proton transfer from acridineH^+ to 1-methylpiperidine. The concentration of 1-methylpiperidine is 4.02×10^9 molecules cm^{-3}, and the temperature is 343 K.

performed assuming pseudo-first-order conditions because the concentration of the neutral reagent B in the ion trap is constant under these conditions and much larger than the concentration of the sample ions (reagent B/sample MH^+ = 10^5−10^6).

Time delays and reagent flows were adjusted to obtain plots that covered two to three half-lives of the reactant ion. The ion trap has been modified to allow for heating of the ion trap and elevated temperatures (343 K) were used in these experiments to reduce ion cluster formation.[16−18] The neutral reagent B is introduced in the same way as in previous studies. Table 1 lists all of the injected ionic reagents (MH^+) and reference compounds (B). The proton affinities of M and B are denoted as PA(M) and PA(B), respectively.

Each rate coefficient was measured three to five times using different reagent flows and partial pressures of the neutral

DOI: 10.1021/jp506913r
J. Phys. Chem. A 2015, 119, 118−126

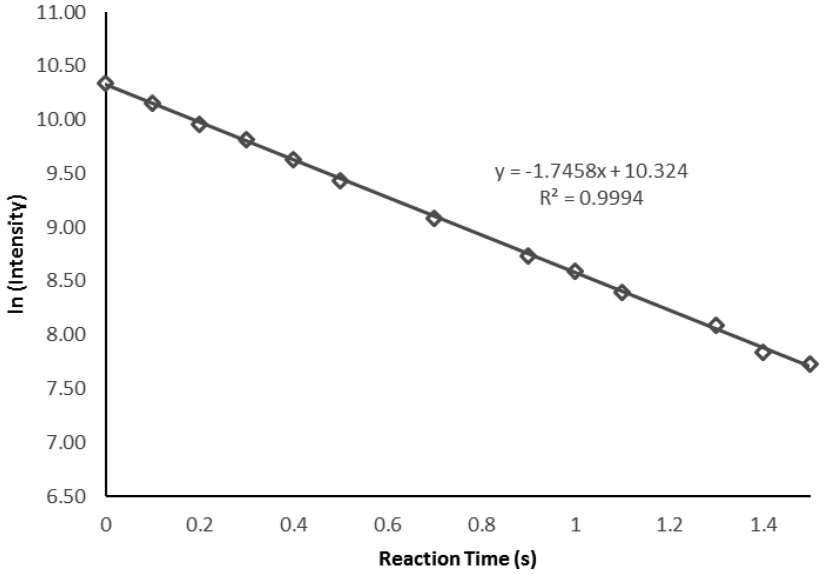

Figure 3. Pseudo-first-order analysis of the reaction of acridineH$^+$ with 1-methylpiperidine. Reaction conditions are the same as for Figure 2.

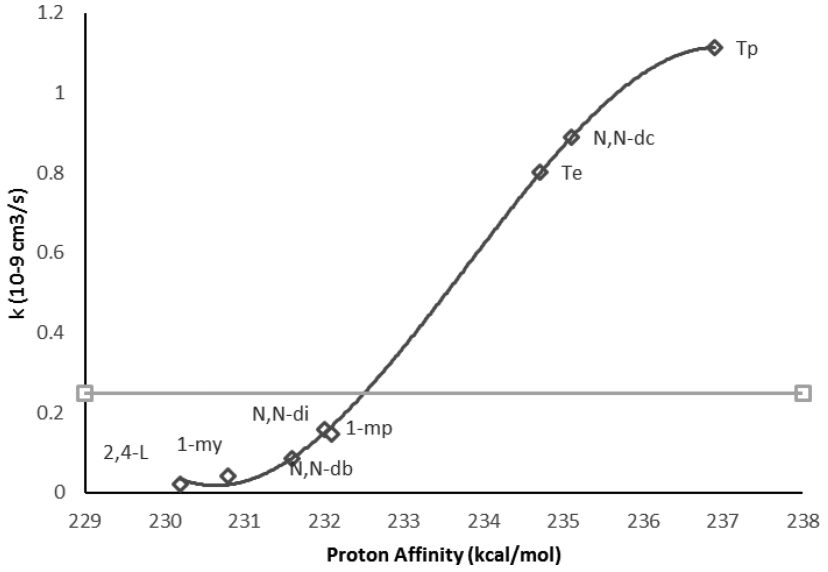

Figure 4. Second-order rate coefficients (10^{-9} cm^3 molecule^{-1} s^{-1}) of proton transfer reactions from acridineH$^+$ to bases B (compound codes in Table 1). The intersection of the horizontal bar at $k = 0.25 \times 10^{-9}$ cm^3 s^{-1} with the sigmoid curve marks the value on the abscissa where PA(M) = PA(B).

reagent. As an example, Figure 2 depicts the raw data from one of four replicate acridineH$^+$ + 1-methylpiperidine proton transfer kinetics measurements. A plot of the natural log of the signal intensity of acridineH$^+$ vs reaction time yields a pseudo-first-order rate constant (k_1), as shown in Figure 3. To obtain second-order rate constants, the pseudo-first-order rate constants were plotted as a function of neutral reagent number density.

COMPUTATIONAL METHODS

The structures of all nitrogen polycyclic aromatic heterocyclic compounds reported in the NIST database,[13,14] and selected other structures were optimized at the B3LYP/6-31G* level of theory. This level of theory was chosen as it is computationally efficient for large molecules and provides reasonably reliable geometries. Single-point energy calculations using these geometries were then performed at the M06-2X/6-311+g** level of theory. Calculations were also performed with the B3LYP/6-311+G**//B3LYP/6-31g* method and with the aug-cc-pvdz basis set, and the calculated PAs by these methods were nearly identical, with an average difference of 0.2 ± 0.4 kcal/mol.[15]

RESULTS

Table 1 lists the second-order rate constants, k_2, for the proton transfer reactions in this study. They were calculated from the experimental pseudo-first-order rate coefficients k_1 and the number densities of neutral reactants B, as described above. The values of k_2 in Table 1 are expressed in units of 10^{-9} cm^3 molecule^{-1} s^{-1}. The reaction efficiencies, $r = k_2/k_{collision}$, can be calculated using $k_{collision}$ from Langevin or average dipole orientation capture rate coefficients.[19] These calculations require the dipole moments and polarizabilities of the neutral reference compounds B, but those properties are not known for

DOI: 10.1021/jp506913r
J. Phys. Chem. A 2015, 119, 118−126

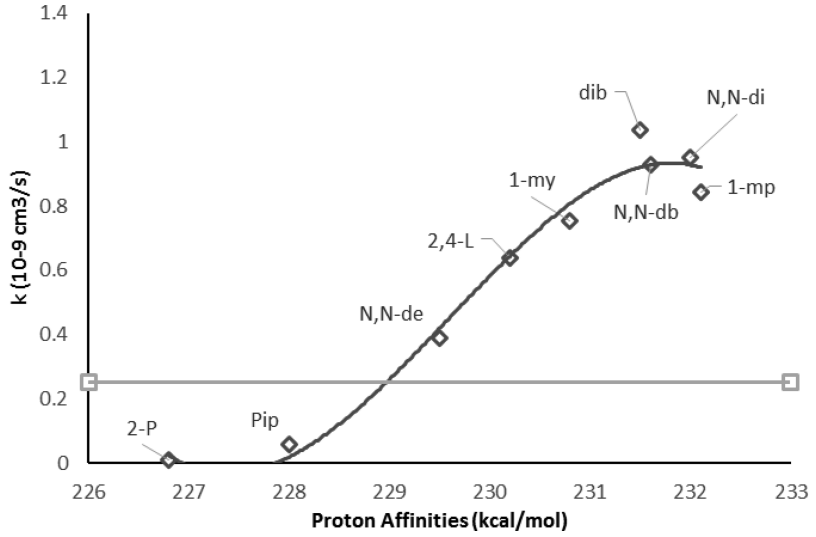

Figure 5. Second-order rate coefficients (10^{-9} cm^3 molecule^{-1} s^{-1}) of proton transfer reactions from dibenzo[*f*,*h*]quinolineH$^+$ to bases B (compound codes in Table 1 and caption of Figure 4).

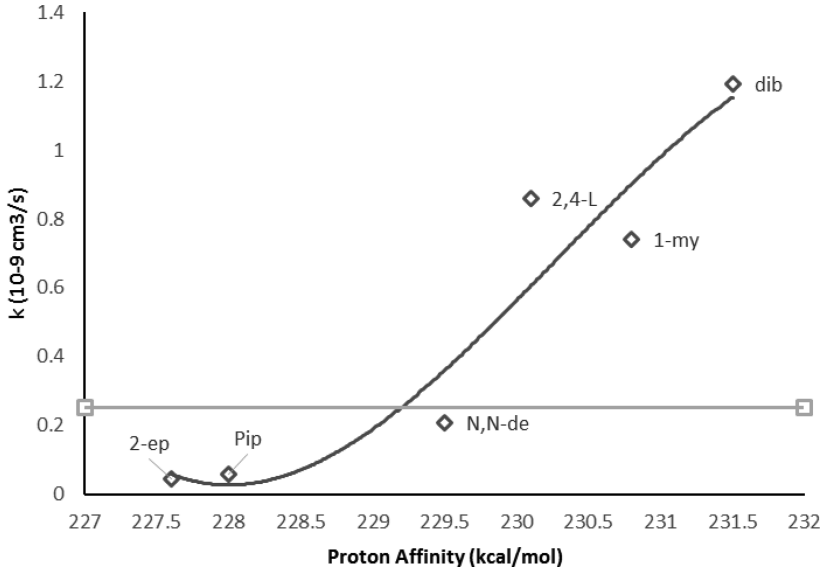

Figure 6. Second-order rate coefficients (10^{-9} cm^3 molecule^{-1} s^{-1}) of proton transfer reactions from phenanthridineH$^+$ to bases B (compound codes in Table 1 and caption of Figure 4).

most of the reference bases B. However, for large organic reactants with large polarizabilities and small dipole moments, the collision rate coefficient is usually 10^{-9} (±30%) cm^3 molecule^{-1} s^{-1}. For this study, we have assumed a collision rate coefficient of 1×10^{-9} cm^3 molecule^{-1} s^{-1} for all the reactions and considered an efficiency of 25% ($k = 2.5 \times 10^{-10}$ cm^3 molecule^{-1} s^{-1}) to indicate an ergoneutral ($\Delta G° = 0$) or thermoneutral ($\Delta H° = 0$) proton transfer process (see below).

Figures 4, 5, and 6 are sigmoid graphs of k_2 vs PA(B). These graphs agree qualitatively with the intrapolation results in Table 1. The intersection of the horizontal bar at $k = 0.25 \times 10^{-9}$ cm^3 s^{-1} with the sigmoid curve marks the value on the abscissa where we assign PA(M) = PA(B). For the other compounds M in Table 1 we applied kinetic bracketing to interpolate to the thermoneutral point, rather than a full plot of slow-to-fast kinetics. Even where a sigmoid curve is available, kinetic bracketing requires only one low and one high bracketing value.

The transition from slow to fast kinetics in Table 1 and in Figures 4, 5, and 6 is fairly sharp, mostly within a range of 2−3 kcal/mol in PA(B). The thermoneutral point where $k_{tn} = 2.5 \times 10^{-10}$ cm^3 molecule^{-1} s^{-1} is defined within ±1 kcal mol^{-1} by interpolation between the nearest points with higher and lower k_2 than k_{tn}. For some compounds, with PA between 232 and 235 kcal/mol, the usable reference compounds were more widely spaced and the thermoneutral points and PA(M) are bracketed within ±1.5 kcal mol^{-1}.

DATA ANALYSIS: KINETIC BRACKETING USING BARRIER-FREE REACTIONS

Kinetic bracketing was applied to obtain thermochemical information from rate coefficients. This is possible where a known quantitative relation exists between kinetics and thermochemistry, such as "intrinsically fast" ion−molecule reactions, including many proton transfer reactions. These reactions have no significant energy barriers and proceed

DOI: 10.1021/jp506913r
J. Phys. Chem. A 2015, 119, 118−126

Table 2. Experimental and Computational GB and PA of Nitrogen Heterocyclics and Reference Bases in the High PA Range[a]

sample M	PA(M) (NIST)[b]	PA(M) exp[c]	PA(M) theory[d]	PA(M) (theory) −PA(M) (exp)[e]	GB_{298} theory[d]	S_{prot} theory[d]
			PANHs			
			One Ring			
pyridine	222.2		220.3	−1.9	212.3	0.4
			Two Rings			
quinoline	227.8		225.7	−2.1	217.7	0.6
isoquinoline	227.5		226.3	−1.2	218.3	0.5
			Three Rings			
acridine	232.5	232.4	232.3	−0.1	224.4	0.7
phenanthridine		228.5	228.4	−0.1	220.4	0.6
benzo[*f*]quinoline		228.6	228.5	−0.1	220.5	0.6
benzo[*h*]quinoline		228.0	226.3	−1.7	218.5	1.2
			Four Rings			
dibenzo[*f*,*h*]quinoline		228.9	227.5	−1.4	219.9	1.9
benzo[*a*]acridine		234.2	233.9	−0.3	226.0	0.7
benzo[*c*]acridine		232.5	231.6	−0.9	223.8	1.3
			Five Rings			
dibenzo[*c*,*h*]acridine		233.0	230.8	−2.2	223.6	3.2
			Reference Bases			
piperidine	228.0		226.8	−1.2	218.9	0.8
2,4-lutidine	230.1		228.9	−1.2	221.2	1.6
N-methylpyrrolidine	230.8		228.9	−1.9	220.0	4.4
1-methylpiperidine	232.1		230.7	−1.4	222.8	0.8
trimethylamine	234.7		233.1	−1.6	224.9	−0.2
tripropylamine	236.9		235.8	−1.1	227.2	−1.3
guanidine	235.7		235.3	−0.4	228.1	3.0
tributylamine	238.6		237.3	−1.3	228.7	−1.8

[a]GB and PA in kcal mol^{-1}, S_{prot} in cal mol^{-1} K^{-1}. [b]Evaluated PA(pyridine) value and literature PAs of quinoline, isoquinoline, and acridine (refs 13 and 14) based on experimental proton transfer equilibrium data in refs 3−7). [c]This work, see Table 1. [d]This work, M06-2X/6-311+g**//B3LYP/6-31G* calculations. [e]Difference between theoretical PAs and experimental PAs for pyridine, quinoline, and isoquinoline from the NIST databases (refs 13 and 14) and for other compounds from present data.

through the same single intermediate in the forward and reverse directions,[20,21] through a single-well potential energy surface. Both the forward and reverse reactions then proceed through the same $(M\cdots H^+\cdots B)^*$ intermediate that can dissociate competitively to form $MH^+ + B$ or $BH^+ + M$. This mechanism, combined with microscopic reversibility and the general relation between equilibrium constants and forward and reverse rate coefficients $K = k_f/k_r$, yields kinetics where the reaction efficiencies are determined fully by the thermochemistry. In these reactions the reaction efficiency r in the forward or reverse directions is determined fully and uniquely by the equilibrium constant $K = \exp(-\Delta G/RT)$ written in the same direction, as in eq 2.[20,21]

$$r = k/k_{collision} = K/(1 + K) \quad (2)$$

Using eq 2, K or $\Delta G = -RT \ln K$ can be determined in principle by measuring the rate coefficient k and calculating or estimating $k_{collision}$. When $T\Delta S$ is small, $\Delta G^\circ_{reaction}$ can be equated with $\Delta H^\circ_{reaction}$ and $\Delta GB = GB(M) - GB(B)$ can be equated with $\Delta PA = PA(M) - PA(B)$. This applies for the present reactions, where the calculated protonation entropies $\Delta S_{prot} = S(MH^+) - S(M)$ for the PANH bases and the reference bases are mostly <2 cal/(mol K) (Table 2). Then, for example, a reaction with an uncertainty of ΔS of ±2 cal mol^{-1} K^{-1} at 343 K leads to an uncertainty $\Delta GB = \Delta PA + T\Delta S \pm 0.7$ kcal mol^{-1} in the difference between the GBs of the sample and reference compounds. Further, for the present reactions, the difference $\Delta GB = GB(M) - GB(B)$ may be equated with $\Delta PA = PA(M) - PA(B)$ within the usual experimental uncertainty of ±1 kcal mol^{-1}.

Historically, bracketing experiments examined whether or not proton transfer from MH^+ to B occurs at observable rates, which brackets $GB(B_{low}) < GB(M) < GB(B_{high})$, where B_{low} and B_{high} are two nearest reference bases to which MH^+ does not or does transfer a proton to B, respectively. In more detailed measurements, kinetic bracketing determines the rate coefficients of reactions 1 using a range of reference bases B to observe the transition from slow to fast kinetics as a function of GB(B). Such transitions were first shown by Bohme et al. in plots of k_{PT} vs GB(B), who used them to measure proton affinities of small molecules.[22,23] Kinetic bracketing was then applied to organic bases, to obtain the proton affinities of alkylbenzene radicals using proton transfer from radical cations to reference bases, and kinetic bracketing was used also to measure the GBs of peptides.[24−26] Subsequently, similar "thermokinetic" plots were applied by Bouchoux and co-workers, who parametrized eq 2 and introduced a correction term corresponding to a small energy barrier of about 0.5 kcal mol^{-1} for nearly ergoneutral reactions,[27] which leads to our assignment of the reaction efficiency $r_{tn} = 0.25$ at the ergoneutral ($\Delta G^\circ_{reaction} = 0$) or thermoneutral ($\Delta H^\circ_{reaction} = 0$) point. Otherwise, for barrier-free single-well reactions at the ergoneutral or thermoneutral points, each collision of $MH^+ + B$ or $BH^+ + M$ would produce a single intermediate $(M\cdots H^+\cdots B)^*$ that dissociates with equal rates to the product BH^+ or to the reactant MH^+, leading to a reaction efficiency of $r_{tn} = 0.5$.

DOI: 10.1021/jp506913r
J. Phys. Chem. A 2015, 119, 118−126

Figures 4, 5, and 6 show such kinetic transition plots for the present reactions. The transition from slow to fast kinetics as GB(B) or PA(B) is relatively sharp over a range of 2−4 kcal mol^{-1} of PA(B). Over this range r varies approximately linearly with PA(B). These plots can be then interpolated according to eq 3 to find the ergoneutral point, here taken where r_{tn} = 0.25 where GB(M) = GB(B) including the Bouchoux correction, or where PA(M) = PA(B) when $\Delta S_{reaction}$ is small. This can usually define GB(M) or PA(M) within ±1 kcal/mol, with an accuracy comparable to the more detailed parametric thermokinetic analysis,[27] but kinetic bracketing requires in principle only two measurements and eq 3 for a simple analysis.

$$\mathrm{GB(B)} = \mathrm{GB(B)}_{low} + ((r_{tn} - r_{low})/(r_{high} - r_{low}))(\mathrm{GB(B)}_{high} - \mathrm{GB(B)}_{low}) \quad (3)$$

Here $\mathrm{GB(B)}_{low}$ and $\mathrm{GB(B)}_{high}$ are the GBs of the nearest reference bases for which the reaction efficiencies are smaller than, or larger than, respectively, r_{tn} = 0.25 as assigned here.

The measured k and the corresponding reaction efficiencies r for reaction 1 in Table 1 increase monotonically with increasing PA(B) of the reference bases as listed in the NIST databases,[13,14] even for relative PAs of ±1 kcal/mol or smaller. This supports that the relative GB/PA values of the reference compounds in the NIST databases are correct within ±1 kcal mol^{-1}, and also that our measured rate coefficients in Table 1 are accurate within the usual ±30% for rate coefficient measurements.

Table 2 also shows calculated GB_{298} values. The contributions of the protonation entropies $S_{prot} = S(MH^+) - S(M)$ at 298 K are small for the rigid compounds M, where only small positive S_{prot} values occur, due mostly to vibrational entropies of the proton in the product MH^+ ions. Given the small S_{prot} values the relative GBs of the PANHs may be equated with the relative PAs for these compounds.

COMPUTATIONAL RESULTS AND COMPARISON WITH EXPERIMENT

The present work aims primarily to define the protonation thermochemistry of PANH compounds. Additionally, it also tests the NIST scale to which the PANH GB/PA results are referenced, which is the largest and most extensively used compilation of GB/PA and ion thermochemistry data.[13,14] In the high GB/PA range above i-C_4H_8 (PA = 191.7 kcal/mol), there are hundreds of biomolecules and superbases, but there are no absolute experimental values from threshold measurements to serve as anchors. Rather, the GB/PA values in the high range are obtained through long equilibrium ladders from lower GB/PAs, and these long extrapolations may be shifted systematically, for example, by uncertainties in experimental temperatures.[13,14,28] Without absolute anchor points, the experimental GB/PA values in the high range may be tested by comparing experiment with theory as was done also for superbasic phosphazenes.[29]

For these comparisons, we note that the uncertainties of the experimental source data values of the NIST scale are usually ±1 kcal/mol, as judged by the consistency of cycles in GB/PA ladders and by the agreement among values from different sources.

As for the PANH compounds, many isomers are not available experimentally, but thermochemical data can be obtained computationally.[15] To evaluate the computational data, we use Table 2 to compare experiment, where available, and theory.

First, for nonaromatic nitrogen bases that we used as reference compounds (bottom section of Table 2), our M06-2X/6-311+G** computational PAs agree with the NIST values within an average (computation − NIST) difference of −1.3 ± 0.5 kcal mol^{-1} with the NIST values;[13,14] i.e., the computed PA values for these nonaromatic nitrogen bases were lower by 1.3 ± 0.5 kcal mol^{-1} than experiment-based NIST values. A similar difference of 1.4 ± 0.9 kcal mol^{-1} between M06-2X/6-311+G** and experiment applies also when these reference bases and the PANH compounds in Table 2, for which NIST values or the present experimental PA values are available, are all considered. The difference between the M06-2X/6-311+G** theoretical results and experiment does not vary systematically with molecular size or with the number or aromatic rings.

It is unlikely that this agreement, nearly within the experimental uncertainty of the NIST database, is caused by a shift from underlying true values independently, in the same direction and by the same amounts, both in the experiment-based NIST database and in the M06-2X/6-311+G** theoretical values. Therefore, this agreement suggests that there is no systematic shift in the NIST scale larger than about ±1 kcal mol^{-1} and that both the NIST values and computations in this range are accurate within ±1.4 kcal mol^{-1} up to 235 kcal/mol. This agreement is significant because there are no experimental anchor PA values above 200 kcal mol^{-1} in this upper range and only theory can provide such independent values.

In comparison, B3LYP/6-311+g**//B3LYP/6-31G* calculations for a larger set of PANHs gave PA values higher by 3.4−4.9 kcal mol^{-1}, and MP2/B3LYP/6-311+g**//B3LYP/6-31G* gave PA values lower by 0.8−2.0 kcal mol^{-1} than the M06-2X/6-311+G** calculations. Unlike M06-2X/6-311+G**, the PAs calculated by these methods differ from experiment from experiment increasingly with molecular size and the number of aromatic rings.[15]

Although close agreement of M06-2X/6-311+G**//B3LYP/6-31g* with experiment supports the NIST upper PA scale, the differences among the various methods suggest that the agreement with experiment may still be coincidental.

Considering these results, a reliable method for calculating the proton affinities of PANH compounds can be by using the M06-2X//6-311+G** computational PA values +1.4 ± 0.9 kcal/mol. These PA values can be then also used to calculate the gas phase basicities, especially the relative gas phase basicities of PANH compounds with similar uncertainties, because the entropies of protonation, and their differences among these compounds are small (Table 2).

APPLICATIONS IN ASTROCHEMISTRY

If PANH compounds are present in interstellar clouds, they can be ionized by radiation or by charge transfer from other ions. In turn, the $PANH^{+\bullet}$ radical ions may then react with H_2 in reactions 4 by hydrogen atom abstraction, with the enthalpy changes as in eq 5, where BDE is the bond dissociation energy and IE is the ionization energy. These reactions are important because they can transform radical cations into less reactive even-electron protonated cations.

$$M^{+\bullet} + H_2 \rightarrow MH^+ + H \quad (4)$$

DOI: 10.1021/jp506913r
J. Phys. Chem. A 2015, 119, 118−126

$$\Delta H^{\circ}_{4} = \mathrm{BDE(H{-}H)} + \mathrm{IE(H)} - \mathrm{IE(M)} - \mathrm{PA(M)} \quad (5)$$

The energy terms for PANH compounds, for which experimental data are available from NIST Webbook or from our measurements, are summarized in Table 3.

Table 3. Energies of Reactions 4 of Hydrogen Atom Transfer from H_2 to $PANH^{+\bullet}$ Ions To Form $(PANH)H^+$ Protonated Ions

M	IE(M) (eV)[a]	PA(M) (kcal/mol)	ΔH°_{4} (kcal/mol)[b]
pyridine	9.26	222.2[a]	−18.0
quinoline	8.63	227.8[a]	−9.0
isoquinoline	8.53	227.5[a]	−6.4
acridine	7.8	232.5[a]	5.4
phenanthridine	8.31	228.5[c]	−2.3
benzo[*h*]quinoline	8.04, 8.3	228.0[c]	4.4
benzo[*a*]acridine	8.1	234.2[c]	−3.2
benzo[*c*]acridine	8.1	232.5[c]	−1.5

[a]From NIST webbook, refs 13 and 14. [b]Calculated from eq 5 using BDE(H−H) = 104.2 kcal/mol and IE(H) = 313.6 kcal/mol. [c]Experimental data from this work.

For compounds larger than two rings, reaction 4 is nearly thermoneutral, or slightly exothermic or endothermic within the uncertainties of the thermochemical data. Further, even the strongly exothermic reaction 4 of pyridine$^{+\bullet}$ with H_2 is slow with rate coefficients of $<10^{-11}$ cm^3 molecule^{-1} s^{-1} at 300−500 K; i.e., the reaction efficiency is <0.01, corresponding, at 300 K, to an energy barrier of >3 kcal/mol, and the temperature dependence of the rate coefficient was also consistent with a similar Arrhenius activation energy.[30] Our preliminary calculations agreed with these experimental observations, indicating a small energy barrier, and showed that the height of the energy barrier depends upon the angle of the incoming H_2 to the pyridine ring. However, we note that calculations of small barriers can have large uncertainties because of the difficulties to identify the transition states and their energies.

In larger molecules, according to the Bell−Evans−Polanyi principle,[31,32] higher barriers may be expected for the less exothermic reactions, and therefore the $(PANH)^{+\bullet}$ radical ions may not be protonated by reactions with H_2 in low temperature 10−50 K interstellar molecular clouds. However, the $(PANH)^{+\bullet}$ ions may become protonated by reactions with other molecules, or with H atoms, as was found for ionized polycyclic aromatic hydrocarbons.[33,34]

CONCLUSIONS

Proton affinities of PANH compounds were determined by kinetic bracketing using the rate coefficients of proton transfer reactions to reference bases in the high PA range. The experimental proton affinities of 1−5-ring polycyclic aromatic nitrogen heterocyclics range from 222 (pyridine) to 234 kcal mol^{-1} (benzo[*a*]acridine) and increase with molecular size and polarizability. Nitrogen in the center rings, and linear ring geometry may also increase the proton affinities. Theoretical M06-2X/6-311+G**//B3LYP/6-31g* calculations closely reproduce the experimental PA's of nonaromatic nitrogen reference bases and 1−5-ring PANH compounds independent of the number of aromatic rings and molecular size. A useful method for calculating the PAs of these compounds can use the computed M06-2X/6-311+G**//B3LYP/6-31g* proton affinities +1.4 ± 0.9 kcal mol^{-1}. Further, the agreement with the experimental values taken from or referenced to the NIST upper GB/PA range suggests that there is no systematic shift in the NIST scale,[13,14] up to 235 kcal/mol, even though there are no absolute anchor points above 200 kcal mol^{-1} in this range.

Also, the rate coefficients of proton transfer from MH^+ to B in our experiments vary monotonically along the NIST relative GB/PA values down to fractions of 1 kcal mol^{-1}. These results also support both the NIST scale and the computations in this high range.

The high GBs/PAs of the PANH bases reflect the dispersal of charge that is transferred from the proton to the hydrocarbon rings of the various ions, in correlation with the polarizabilities of these molecules. The GBs/PAs can be also affected by the molecular geometry and the location of the ring nitrogen, and by the presence of further nitrogen atoms in multinitrogen PANHs.[15]

The H atom transfer reactions from H_2 to the present 3−5-ring $(PANH)^{+\bullet}$ are nearly thermoneutral. For pyridine$H^{+\bullet}$ this reaction has a small barrier that may be similar to or larger than those of the less exothermic reactions of larger $PANH^{+\bullet}$ + H_2 systems. These reactions with energy barriers would be slow at low temperatures, which allows these reactive $PANH^{+\bullet}$ radical ions to persist in cold interstellar clouds.

We are continuing further investigations, both experimentally and theoretically, of structural effects on the intrinsic gas-phase basicities of PANH compounds, and of their astrochemical applications.

AUTHOR INFORMATION

Notes

The authors declare no competing financial interest.

ACKNOWLEDGMENTS

We thank Mr. David Derkits for preliminary measurements of proton transfer kinetics. S.G. acknowledges the National Science Foundation for support (CHE-1300817).

REFERENCES

(1) Taft, R. W. Protonic Acidities and Basicities in the Gas Phase and in Solution: Substituent and Solvent Effects. *Prog. Phys. Org. Chem.* **1983**, *14*, 247−350.

(2) Taft, R. W.; Anvia, F.; Taagepera, M.; Catalan, J.; Elguero, J. Electrostatic Proximity Effects in the Relative Basicities and Acidities of Pyrazole, Imidazole, Pyridazine, and Pyrimidine. *J. Am. Chem. Soc.* **1986**, *108*, 3237−3239.

(3) Aue, D. H.; Webb, H. M.; Davidson, W. R.; Toure, P.; Hopkins, H. P., Jr.; Moulik, S. P.; Jahagirdart, J. V. Relationships Between the Thermodynamics of Protonation in the Gas and Aqueous Phase for 2-, 3-, and 4-Substituted Pyridines. *J. Am. Chem. Soc.* **1991**, *113*, 1770−1780.

(4) Aue, D. H.; Webb, H. M.; Bowers, M. T. Quantitative Proton Affinities, Ionization Potentials, and Hydrogen Affinities of Alkylamines. *J. Am. Chem. Soc.* **1976**, *98*, 311−317.

(5) Davidson, W. R.; Sunner, J.; Kebarle, P. Hydrogen Bonding of Water to Onium Ions. Hydration of Substituted Pyridinium Ions and Related Systems. *J. Am. Chem. Soc.* **1979**, *101*, 1675−1680.

(6) Lau, Y. K.; Saluja, P.P. S.; Kebarle, P.; Alder, R. W. Gas-Phase Basicities of N-Methyl Substituted 1,8-Diaminonaphthalenes and Related Compounds. *J. Am. Chem. Soc.* **1978**, *100*, 7328−7334.

(7) Meot-Ner (Mautner), M. Ion Thermochemistry of Low-Volatility Nitrogen Heterocyclics and Nucleic Bases. *J. Am. Chem. Soc.* **1979**, *101*, 2396−2403.

DOI: 10.1021/jp506913r
J. Phys. Chem. A 2015, 119, 118−126

(8) Elsila, J. E.; Hammond, M. R.; Bernstein, M. P.; Sandford, S. A.; Zare, R. N. UV Photolysis of Quinoline in Interstellar Ice Analogues. *Meteorit. Planet. Sci.* **2006**, *41*, 785−796.
(9) Hudgins, D. M.; Bauschlicher, C. W.; Allamandola, L. J. Variations in the Peak Position of the 6.2 μm Interstellar Emission Feature: A Tracer of N in the Interstellar Polycyclic Aromatic Hydrocarbon Population. *Astrophys. J.* **2005**, *632*, 316−332.
(10) Mattioda, A. L.; Hudgins, D. M.; Bauschlicher, C. W.; Rosi, M.; Allamandola, L. J. Infrared Spectroscopy of Matrix-Isolated Polycyclic Aromatic Compounds and Their Ions. 6. Polycyclic Aromatic Nitrogen Heterocycles. *J. Phys. Chem. A* **2003**, *107*, 1486−1498.
(11) Boersma, C.; Bregman, J. D.; Allamandola, L. J. Properties of Polycyclic Aromatic Hydrocarbons in the Northwest Photon Dominated Region of NGC 7023. I PAH Size, Charge, Composition, and Structure Distribution. *Astrophys. J.* **2013**, *769*, 117.
(12) Steel, P. J. Ligand Design in Multimetallic Architexture: Six Lessons Learned. *Acc. Chem. Res.* **2005**, *38*, 243−250.
(13) Hunter, E. P. L.; Lias, S. G. Evaluated Gas Phase Basicities and Proton Affinities of Molecules: An Update. *J. Phys. Chem. Ref. Data* **1998**, *27*, 413−652.
(14) Hunter, E. P.; Lias, S. G. Proton Affinity Evaluation. In *NIST Chemistry WebBook*; Linstrom, P. J., Mallard, W. G., Eds.; NIST Standard Reference Database Number 69; National Institute of Standards and Technology: Gaithersburg, MD, 20899, http://webbook.nist.gov (retrieved May 24, 2014).
(15) Maclagan, R. G. A. R.; Gronert, S.; Meot-Ner (Mautner), M. Protonated Polycyclic Aromatic Nitrogen Heterocyclics: Proton Affinities, Polarizabilities, and Atomic and Ring Charges of 1−5-Ring Ions. *J. Phys. Chem. A* **2015**, DOI: 10.1021/jp5069939.
(16) Gronert, S.; Fagin, A. E.; Okamoto, K.; Mogali, F.; Pratt, L. M. Leaving Group Effects in Gas-Phase Substitutions and Eliminations. *J. Am. Chem. Soc.* **2004**, *126*, 12977−12983.
(17) Gronert, S. Quadrupole Ion Trap Studies of Fundamental Organic Reactions. *Mass Spectrom. Rev.* **2005**, *24*, 100−120.
(18) Derkits, D.; Lamp, J.; Harge, J.; Snead, R. S.; Wiseman, A.; Gronert, S. Variable Temperature Ion Trap Mass Spectrometer for the Study of Gas-Phase Reactions. *Am. Soc. Mass Spectrom. Conf.*, Minneapolis, Minnesota **2013**.
(19) Su, T.; Chesnawich, W. J. Parametrization of the Ion-Polar Molecule Collision Rate Constant by Trajectory Calculations. *J. Chem. Phys.* **1982**, *76*, 5183−5185.
(20) Sieck, L. W.; Meot-Ner (Mautner), M. Ionization Energies and Entropies of Cycloalkanes. Kinetics of Free-Energy Controlled Charge Transfer Reactions. *J. Phys. Chem.* **1982**, *86*, 3646−3650.
(21) Meot-Ner (Mautner), M. Entropy-Driven Proton Transfer Reactions. *J. Phys. Chem.* **1991**, *95*, 6580−6585.
(22) Bohme, D. K.; Mackay, G. I.; Schiff, H. I. Determination of Proton Affinities from the Kinetics of Proton Transfer Reactions. VII. The proton affinities of O_2, H_2, Kr, O, N_2, Xe, CO_2, CH_4, N_2O, and CO. *J. Chem. Phys.* **1980**, *73*, 4976−4986.
(23) Roche, A. E.; Sutton, M. M.; Bohme, D. K. Determination of Proton Affinity from the Kinetics of Proton Transfer Reactions. 1. Relative Proton Affinities. *J. Chem. Phys.* **1971**, *55*, 5480−5484.
(24) Meot-Ner (Mautner), M. Carbon-Hydrogen Bond Dissociation Energies in Alkylbenzenes. Proton Affinities of the Radicals and the Absolute Proton Affinity Scale. *J. Am. Chem. Soc.* **1982**, *104*, 5−10.
(25) Shen, J.; Brodbelt, J. S. Evaluation of Proton-Binding Capabilities of Polyether and Pyridyl Ligands. *J. Mass Spectrom.* **1998**, *33*, 118−129.
(26) Reyzer, M. L.; Brodbelt, J. S. Gas-Phase Basicities of Polyamines. *J. Am. Soc. Mass Spectrom.* **1998**, *9*, 1043−1048.
(27) Bouchoux, G.; Salpin, J. Y.; Leblanc, D. A Relationship Between the Kinetics and Thermochemistry of Proton Transfer Reactions in the Gas Phase. *Int. J. Mass Spectrom. Ion Processes* **1996**, *153*, 37−48.
(28) Meot-Ner (Mautner), M. The Proton Affinity Scale, and Effects of Ion Structure and Solvation. *Int. J. Mass Spectrom.* **2003**, *127*, 525−554.
(29) Kaljurand, I.; Koppel, I. A.; Kutt, A.; Room, E. I.; Rodima, T.; Koppel, I.; Mishima, M.; Leito, I. Experimental Gas-Phase Basicity Scale of Superbasic Phosphazenes. *J. Phys. Chem. A* **2007**, *111*, 1245−1250.
(30) Attah, K. I.; Platt, S.; El-Shall, M. S.; Maclagan, R. G. A. R.; Meot-Ner (Mautner), M. Personal communication, 2014.
(31) Evans, M. G.; Polanyi, M. Some Applications of the Transition State Method to the Calculation of Reaction Velocities, Especially in Solution. *Trans. Faraday Soc.* **1935**, *31*, 875−894.
(32) Evans, M. G.; Polanyi, M. Inertia and Driving Force of Chemical Reactions. *Trans. Faraday Soc.* **1938**, *34*, 11−24.
(33) Snow, T. P.; Le Page, V.; Keheyan, Y.; Bierbaum, V. M. The Interstellar Chemistry of PAH Cations. *Nature* **1998**, *391*, 259−260.
(34) LePage, V.; Snow, T. P.; Bierbaum, V. M. Hydrogenation and Charge States of Polycyclic Aromatic Hydrocarbons in Diffuse Clouds. II. Results. *Astrophys. J.* **2003**, *584*, 316−330.

DOI: 10.1021/jp506913r
J. Phys. Chem. A 2015, 119, 118−126